Supporting Information

Evidence for Lower Critical Solution Behaviour in Ionic Liquid Solutions

Joanna Lachwa, Jerzy Szydlowski, Vesna Najdanovic-Visak, Luís P.N. Rebelo*, Kenneth R. Seddon*, Manuel Nunes da Ponte, José M.S.S. Esperança, Henrique J.R. Guedes

Instituto de Tecnologia Química e Biológica, UNL, Av. República, Ap. 127, 2780-901 Oeiras, Portugal, and The QUILL Centre, The Queen's University of Belfast, Stranmillis Road, Belfast BT9 5AG, U. K.

* luis.rebelo@itqb.unl.pt and k.seddon@qub.ac.uk

Experimental

Chemicals. 1-alkyl-3-methylimidazolium bis{(trifluoromethyl)sulfonyl}amide, $[C_n mim][NTf_2]$, with n ranging from 2 to 10, were synthesised at QUILL (The Queen's University Ionic Liquid Laboratories, Belfast) according to methods found elsewhere,[1] where they underwent first-stage purification. These ionic liquids were washed several times with water to decrease the chloride content. It was confirmed that no precipitation (of AgCl) would occur by adding $AgNO_3$ to the wash water. NMR analyses showed no major impurities in the untreated, original samples, except for the presence of water. All samples were further thoroughly degassed, dried, and freed from any small traces of volatile compounds by applying vacuum (0.1 Pa) at moderate temperatures (60 - 80ºC) for typically 48 h. Then, both the water and chloride contents were analysed. Karl-Fischer titrations revealed very low levels of water (below 70 ppm) for all treated ILs to be compared with values of 2500 – 5500 ppm of water for untreated samples. The Cl^- specific electrode using the standard addition method has generally shown chloride contents in the range of 20-150 ppm. In this work, only $[C_4 mim][NTf_2]$ and $[C_5 mim][NTf_2]$ were used. Trichloromethane (99.9+%, HPLC grade) and tetrachloromethane (99.9+%, HPLC grade) were purchased from Sigma-Aldrich. Both were further dried with 3 Å molecular sieves. All liquid mixtures were gravimetrically prepared to an estimated uncertainty of 0.02 weight %.

Apparatus for Liquid-liquid Phase Transitions. Both light scattering techniques and visual detection of phase transitions were used. As for the first, phase diagrams were obtained with a He-Ne laser light scattering apparatus, which operates up to pressures of 50 bar. It contains a thick-walled Pyrex glass tube cell (internal volume ~ 1.0 cm^3, optical length ~ 2.6 mm) connected to a pressure line and separated from it by a mercury plug. The apparatus, as well as the methodology used for the determination of phase transitions, have recently been described in detail elsewhere.[2] Here, only a brief description is provided. Scattered light intensity (I_{sc}) is captured at a very low angle ($2 < 2\theta /° < 4$) in the outer part of a bifurcated optical cable, while transmitted light (I_{tr}) is captured in the inner portion of this cable. Intensities are corrected for density fluctuations, reflections, and multiple scattering effects. The cloud-point is the point on the $(I_{sc,corr})^{-1}$ against pressure (p) or temperature (T) least-squares fits where the slope changes abruptly. Temperature accuracy is typically ± 0.01 K in the range $240 < T/K < 400$. As for pressure, accuracy is ± 0.1 bar. The cell can be operated in the isobaric or isothermal mode. In this work, this apparatus was mainly used for the determination of phase transitions at pressures different from the atmospheric one.

With the naked eye, nominal atmospheric pressure determinations, first, turbidity (as a sign for a cloud-point), and, then, clearly visible separation of the two phases was observed in sealed Pyrex glass capillaries (~ 0.5 cm^3) containing small stirrers. Very small dead volumes of gas phase were allowed to coexist with the liquid in order to avoid corrections to composition due to vaporization. Usually, LCST-transitions were obtained by slow temperature increase (typically, 2 K per hour) of a glass-walled bath filled with ethanol and liquid nitrogen (for temperatures between 213 K and 293 K), water (from 293 K up to 343 K), or silicon oil (up to 480 K). For UCST-type of transitions, either this methodology was maintained – in which case one looks for the disappearance of the last small drop of the second phase – or one starts in the homogeneous region and further slowly cools off the bath. Temperature (estimated accuracy ~ 0.02 K) was measured with a calibrated platinum resistance thermometer coupled to a high-precision multimeter. The accuracy of the transition temperatures is worse as it also depends on the

purity of chemicals, rate of temperature change, as well as on the visual criterion to define the transition point.

Mass Spectrometry. The electro-spray mass spectra were performed on an ion trap instrument (Brucker, model Esquire 3000+, with upper mass to charge (m/z) limit of 3000 Da) in the positive and negative modes for [C_4mim][NTf$_2$] and [C_5mim][NTf$_2$] using trichloromethane, CHCl$_3$, as the solvent at an approximate dilution of 1:1000, flow rate of 100 μL/h, and source temperature of 200 ºC. As an example, the spectra of [C_5mim][NTf$_2$] are shown in Figure S1.

Results and Brief Thermodynamic Interpretation

Two distinct types of liquid-liquid phase splitting upon temperature increase have been found. One of them is the result of relatively strong, oriented interactions between the IL and the organic solvent; the other emerges whenever the solvent is significantly expanded compared to the IL. In two of the cases investigated, both types of demixing are present in the same phase diagram, which constitutes the first experimental support for the existence of a recently theoretically postulated [3,4] special kind of type-VII phase diagram. Transition temperatures are illustrated in Figure 1 (main text), as well as Figure S2 for their pressure dependence.

Liquid-liquid phase separation occurs whenever a critical, almost-always-positive value of the excess Gibbs energy of mixing (g^E) is reached and over-taken[5] [in a simplified notation, $g^E/RTx(1-x) \geq g_c > 0$] – see also Figure 2 (main text). In turn, and under some restrictive assumptions,[5-7] it is a thermodynamic requirement that the homogeneous mixture in the vicinity of a lower critical solution temperature (LCST) is formed upon the exothermic mixing ($\Delta h = h^E < 0$) of its constituents. Consequently, only a superimposing (negative) entropic contribution ($s^E < 0$) can justify its occurrence ($g^E = h^E - Ts^E$). Thus, there is an underlying structuring effect upon mixing in excess of the (positive) change of the entropy of ideal mixing ($\Delta s = s^E + \Delta s^{id}$).

The liquid-liquid LCST-type of demixing is almost exclusive of a few aqueous solutions and/or polymeric ones. Usually, in the first case, strong, oriented interactions especially those between unlike species intervene (typically, H-bonds), while in the second, most of the systems are composed of weakly interacting segmental portions. Commonly, there are, thus, two distinct mechanisms that may be responsible for the occurrence of a LCST. One of them is related to the formation and disruption of strong interactions, and the other is connected to a different phenomenon. The above-mentioned weakly interacting systems are usually composed of species visibly different in size (*e.g.*, polymer + small molecule). Here, at relatively high temperatures, while the larger component has a relatively low expansivity, the smaller (more volatile) one can be highly expanded. Therefore, upon mixing, the small molecule system contracts significantly producing a decrease in the entropy of the system. Both distinct mechanisms share an exothermic process upon mixing. In contrast, critical phase separation phenomena that occur as temperature is lowered are accompanied by endothermic processes ($\Delta h = h^{E} > 0$) – upper critical solution temperature (UCST). This is by far the most commonly encountered phenomenon in demixing processes. A closed-loop phase diagram contains an UCST at a higher temperature than the LCST.

The inserts in Figure 1 (main text) share the phase diagram of the binary $[C_5mim][NTf_2]$ + $CHCl_3$, but in system **II** the solvent quality of the substituted chlorinated methane is varied (mixtures of $CHCl_3$ + CCl_4, forming the hypothetical solvent CH_xCl_{4-x}, where $0 < x \leq 1$). The lower solvent ability of CCl_4 compared to that of $CHCl_3$ induces the decrease of the LCST and the appearance of the UCST as the ratio $CCl_4/ CHCl_3$ subtly increases.

It should be noted that at the merging points of UCSTs and LCSTs (double critical points), $\partial T_c/\partial m$, $\partial T_c/\partial x$, $\partial T_c/\partial p$, *etc.*, tend to infinity – see also Figure S2. This is why tiny changes in any of these field variables provoke dramatic shifts in the phase behaviour.

Both systems (**I** and **II**) represented in Figure 1 most probably express potentially similar phase behaviour – special kind of type VII - although the second LCST [$LCST_1$] of the latter, which would

form a closed-loop, is hidden in the region of overly low temperatures (where solidification has already occurred). Therefore, system **II** reveals a type IV behaviour.

Phase behaviour as that depicted for system **I** in Figure 1 has never been found. The best approximation is that found for water + 2-butanol at high pressure [3,8] but, in fact, the situation is reversed. It presents a normal low-temperature demixing (UCST) and a closed loop at high temperatures. Moreover, to the best of our knowledge, both systems investigated in this work represent the first published findings of LCST behaviour in binary and *quasi*-binary IL systems, with or without the presence of a closed-loop.

To date, the information so far accumulated on binary L-L phase diagrams that depict phase separation of solutions of IL + solvent, permits us to identify the phase diagrams as belonging to two major classes: (i) partially immiscible and (ii) UCST – see Figure S3. In the first case, the situation most commonly encountered is one in which the solvent dissolves to a certain extent in the IL, whereas the IL practically does not dissolve in the solvent. Also, the solvent dissolves better in the IL as temperature rises. In the UCST-type of phase diagrams, there is partial mutual solubility at low temperatures [as in case (i)], which transforms itself into total mutual miscibility above a certain higher temperature (L-L critical temperature). These two kinds [(i) and (ii)] of phase diagrams do in fact belong to the same type-II of phase diagram.[13] Note that, in case (i) either vaporisation of the solvent and/or degradation of the IL as temperature rises will occur, preventing us from detecting a potentially existent critical point at high temperatures (see Figure S3). Interestingly, to the best of our knowledge, UCST-type phase diagrams in IL + solvent so far have only been found for cases where the solvent is either water or an alcohol.[9-12]

Although not strictly belonging to the case of binary and *quasi*-binary mixtures, IL-containing liquid solutions in which phase splitting is provoked (or the two-phase domain is augmented) by the addition of an inorganic salt to a (water + IL) mixture [14] is worth mentioning. This phenomenon constitutes the so-called "salting-out" or water-structuring salt effect, and is provoked by increasing the ionic strength of the solution.

A common feature of basically all experimental phase diagrams of ionic liquid containing mixtures is that the critical composition is found at low values of IL composition, lower than those expected by direct consideration of an ionic-pair type of structure. This fact underlies the possibility that ILs, even in solution, tend to form aggregates (typically three-dimensional polymer-like supramolecules stabilized by specific, oriented interactions). This is supported both by independent experimental evidence as well as theoretical deduction. For instance, it is relatively easy to demonstrate [5,7] that within the frame of simple lattice-like models binary mixtures constituted by identical size species present a critical mole fraction, x_c, equal to 0.5, and, that the critical value of the excess Gibbs energy that provokes phase separation is $g^E/RTx(1-x) \geq g_c = 2$. As one moves to systems composed of unlike molecules of very distinct sizes (*e.g.*, polymer + small molecule) the critical mole fraction of the largest component, x_{1c}, decreases together with the critical value, g_c, necessary to induce phase separation,

$$x_{1,c} = \frac{1}{1+r^{3/2}} \; ; \qquad\qquad g_c = \frac{1}{2}\left(1+\frac{1}{r^{1/2}}\right)^2$$

where r represents, in first approximation, the ratio of sizes of the two components.

Related Systems. To emphasize the discussion posed in the last paragraph of the main text, we are currently experimentally confirming that, in fact, $[NTf_2]^-$-based ILs can phase separate from their solutions upon temperature increase in systems with solvents containing aromatic rings, especially for short alkyl chain substitutes in the imidazolium cation. The underlying specific interactions between the IL and solvents such as benzene, toluene, *etc.*, brought about by the presence of π-clouds, have recently been found for the case of benzene.[15,16] In our investigations, as the imidazolium alkyl chain of the IL increases the mixtures containing either benzene, toluene, or α-methylstyrene, evolve from an "abnormal" high-temperature demixing behaviour to the common one of phase splitting as temperature diminishes (UCST). Other experimental determinations of L-L phase splitting in (IL + aromatic) mixtures reported in the literature [17] show partial miscibility as depicted in Figure S3. In some cases, clathrate formation has been found. [15] Interestingly, it has been reported [18] that, whereas the partial molar excess enthalpy of infinitely diluted benzene in $[C_2mim][NTf_2]$ is negative (*ca.* -600 J mol^{-1}), that

of its non-aromatic counterpart (cyclohexane) in the same IL is positive (approx. +6 kJ mol^{-1}). This distinct behaviour has been pointed out as evidence for the potential use of ILs as entrainers for the separation of aromatic from aliphatic hydrocarbons in extraction processes.

References

(1) Bonhôte, P.; Dias. A.-P.; Armand, M.; Papageorgiou, N.; Kalyanasundaram, K.; Gratzel, M. *Inorg. Chem.* **1996**, *35*, 1168-1178.

(2) de Sousa, H.C.; Rebelo, L.P.N. *J. Chem. Thermodyn.* **2000**, *32*, 355-387.

(3) Schneider, G.M. *Phys. Chem. Chem. Phys.* **2002**, *4*, 845-852, and references therein.

(4) (a) Yelash, L.V.; Kraska, T. *Ber. Bunsenges. Phys. Chem.* **1998**, *102*, 213-223; (b) Bolz, A.; Deiters, U.K.; Peters, C.J.; de Loos, T.W. *Pure Appl. Chem.* **1998**, *70*, 2233-2257.

(5) Rebelo, L.P.N. *Phys. Chem. Chem. Phys.* **1999**, *1*, 4277-4286 and references therein.

(6) Progine, I.; Defay R. *Chemical Thermodynamics* (transl. Everett, D.H.), Longmans Green, London, **1954**, pp. 271-290.

(7) Schneider, G. *Ber. Bunsen. Phys. Chem.* **1966**, *70*, 497-520.

(8) Walker, J.S.; Vause, C.A. *Sci. Am.* **1987**, *256*, 90-97.

(9) Crosthwaite, J.M.; Aki, S.N.V.K.; Maginn, E.J.; Brennecke, J.F. *J. Phys. Chem. B* **2004**, *108*, 5113-5119.

(10) Najdanovic-Visak, V.; Esperança, J.M.S.S.; Rebelo, L.P.N.; Nunes da Ponte, M.; Guedes, H.J.R.; Seddon, K.R.; de Sousa, H.C.; Szydlowski, J. *J. Phys. Chem B* **2003**, *107*, 12797-12807.

(11) Wagner, M.; Stanga, O.; Schröer, W. *Phys. Chem. Chem. Phys.* **2003**, *5*, 3943-3950.

(12) (a) Najdanovic-Visak, V.; Esperança, J.M.S.S.; Rebelo, L.P.N.; Nunes da Ponte, M.; Guedes, H.J.R.; Seddon, K.R.; de Sousa, H.C.; Szydlowski, J. *Phys. Chem. Chem. Phys.*, **2002**, *4*, 1701-1703; (b) Swatloski, R.P.; Visser, A.E.; Reichhert, W.M.; Broker, G.A.; Farina, L. M.; Holbrey J.D.; Rogers, R.D. *Chem. Commun.*, **2001**, 2070-2071; (c) Wu, C.–T.; Marsh, K.N.; Deev A.V.; Boxall, J. A. *J. Chem. Eng. Data*, **2003**, *48*, 486-491; (d) Marsh, K.N.; Deev A.V.; Wu, A.C.–T.; Tran, E.; Klamt, A. *Korean J. Chem. Eng.*, **2002**, *19*, 357-362; (e) Heintz, A.; Lehmann, J.K.;

Wertz, C. *J. Chem. Eng. Data*, **2003**, *48*, 472-474; (f) Swatloski, R.P.; Visser, A.E.; Reichhert, W.M.; Broker, G.A.; Farina, L. M.; Holbrey J.D.; Rogers, R.D. *Green Chem.* **2002**, *4*, 81-87; (g) Döker, M.; Gmehling, J. *Fluid Phase Equilib.* **2005**, *227*, 255-266.

(13) van Konynenburg, P.H.; Scott, R.L. *Phil. Trans.* **1980**, *298*, 495-540.

(14) Gutowski, K.E.; Broker, G.A.; Willauer, H.D.; Huddleston, J.G.; Swatloski, R.P.; Holbrey, J.D.; Rogers, R.D. *J. Am. Chem. Soc.* **2003**, *125*, 6632-6633.

(15) Holbrey, J.D.; Reichert, W.M.; Nieuwenhuyzen, M.; Sheppard, O.; Hardacre, C.; Rogers, R.D. *Chem. Comm.* **2003**, 476-477.

(16) Deetlefs, M.; Hardacre, C.; Nieuwenhuyzen, M.; Sheppard, O.; Soper, A. *J. Phys. Chem. B* **2005**, *109*, 1593-1598.

(17) (a) Blanchard, L.A.; Brennecke, J.F. *Ind. Eng. Chem. Res.* **2001**, *40*, 287-292; (b) Domanska, U. *Pure Appl. Chem.* **2005**, *77*, 543-557; (c) Domanska, U.; Marciniak, A. *J. Chem. Eng. Data* **2003**, *48*, 451-456, (d) Kato, R.; Krummen, M.; Gmehling, J. *Fluid Phase Equilib.* **2004**, *224*, 47-54; (e) Letcher, T.M.; Deenadayalu, N. *J. Chem. Thermodyn.* **2003**, *35*, 67-76; (f) Domanska, U.; Mazurowska, L. *Fluid Phase Equilib.* **2004**, *221*, 73-82.

(18) Krummen, M.; Wassercheid, P.; Gmehling, J. *J. Chem. Eng. Data* **2002**, *47*, 1411-1417.

(19) Although normal boiling temperatures of ILs are experimentally unknown, estimates for them ($T_{eb,IL}$) have just become available. [20]

(20) Rebelo, L.P.N.; Canongia Lopes, J.N.; Esperança, J.M.S.S.; Filipe, E. *J. Phys. Chem. B* **2005**, *109*, 6040-6043.
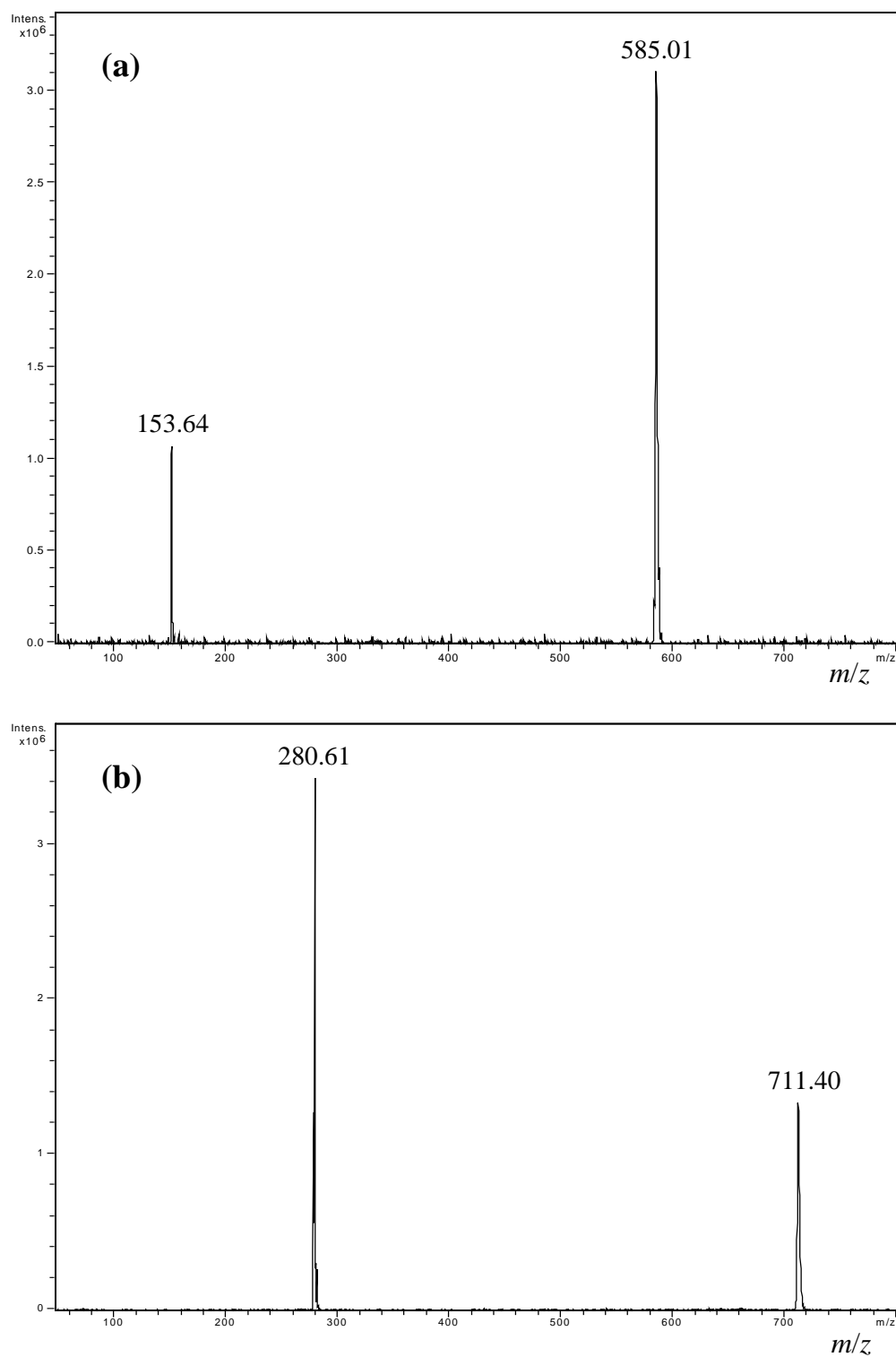
Figure S1. ESI-MS in the positive (a) and negative (b) modes of [C$_5$mim][NTf$_2$] in trichloromethane (dilution of 1:1,000). Intensity versus (*m/z*).
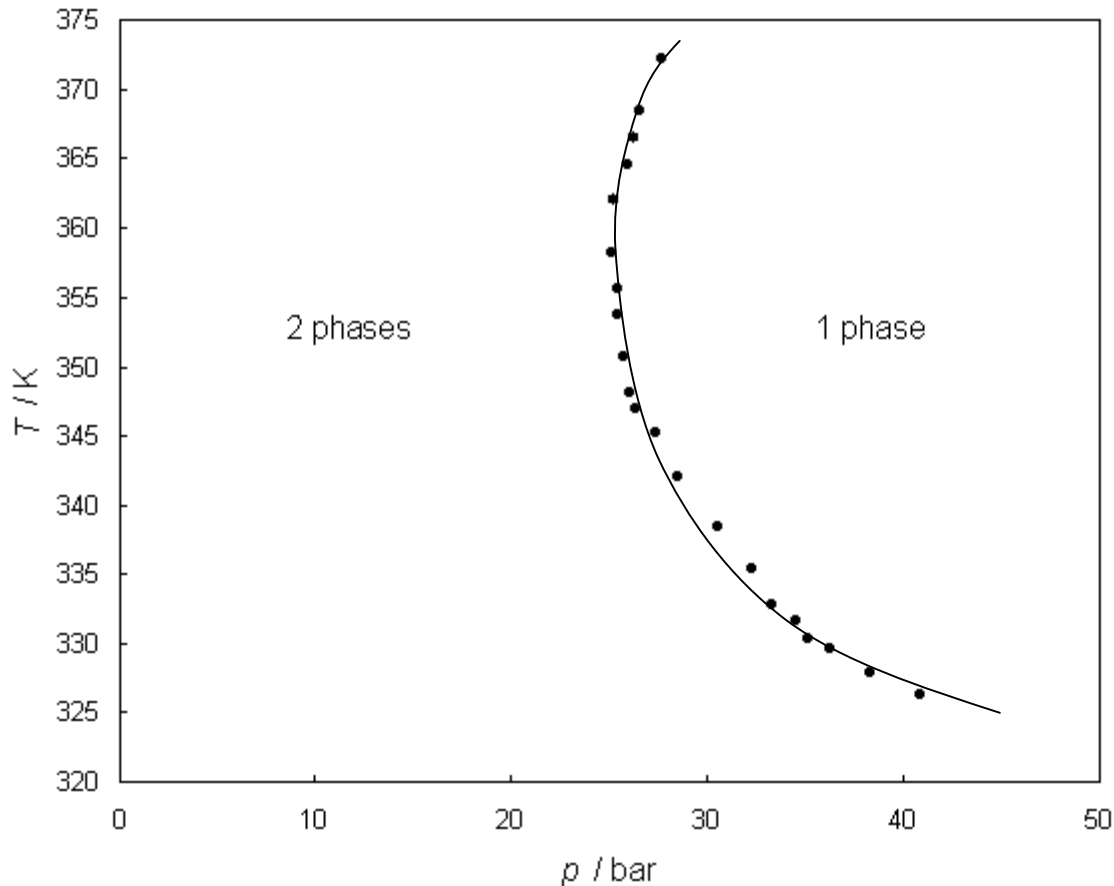
Figure S2. Liquid-liquid equilibrium temperatures as a function of pressure for the concentration w_{IL} = 0.1362 and m = 4.320 of ([$C_m$mim][NTf$_2$] + CHCl$_3$); w_{IL} is the weight fraction of the hypothetical ionic liquid [$C_m$mim][Ntf$_2$], where m is the average number of carbons in the alkyl chain of the cation; •, experimental data. The upper and lower parts of the curve defined by the experimental points correspond to the pressurised LCST$_2$ and UCST branches, respectively, of the phase diagram of Fig. 1 - system **I** (which was obtained at a nominal pressure of 1 bar). The pressurised, low-temperature LCST$_1$ branch is not shown in the figure. Note the infinite slope at the merging point (double critical point) of the LCST$_2$ and UCST.
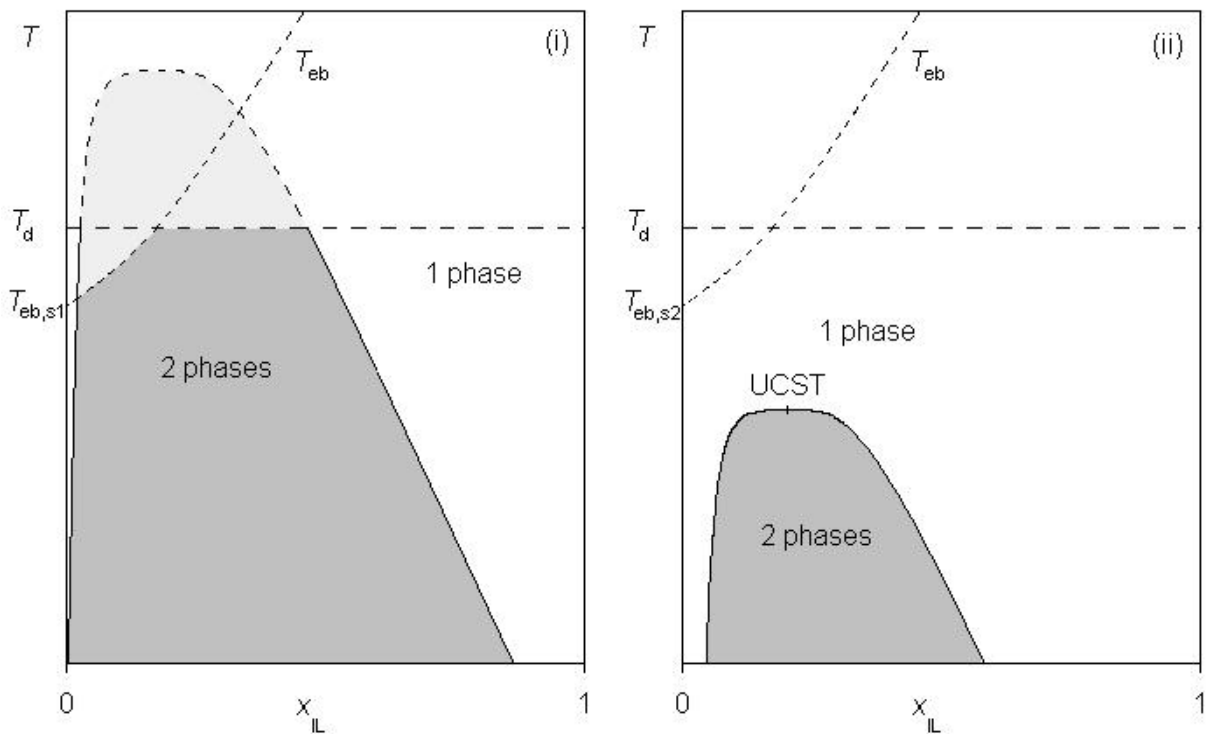
Figure S3. Schematic, commonly encountered L-L phase diagrams in binary (IL + solvent) mixtures at a nominal pressure of 1 bar. T_{eb}, boiling temperature of the mixture; T_{eb} (s_1 or s_2), boiling temperature of the pure solvent; $T_{eb,IL}$, boiling temperature of the pure IL (located at much higher temperatures, and, thus, not shown in the plots [19,20]); T_d, decomposition temperature of the IL; UCST, upper critical solution temperature. Case (i) represents situations in which the solvent (s_1) quality for the mixing with the IL is worse than in case (ii) – s_2. In case (i) the upper branch of the binodal L-L curve is interrupted by either the boiling of the mixture and/or the decomposition of the IL. Therefore, the light-grey region is experimentally inaccessible.